Available free online at www.medjchem.com

Mediterranean Journal of Chemistry **2015**, 4(2), 68-80

Role of activated carbon on micropollutants degradation by different radiation processes

Inmaculada Velo-Gala, Jesús J. López-Peñalver*, Manuel Sánchez-Polo and José Rivera-Utrilla

Department of Inorganic Chemistry, Faculty of Science, Granada University, Granada, Spain

Abstract: This work supplements our previous studies, but in this work, we stress the ability of activated carbon by itself to stabilize the radicals formed in advanced oxidation processes. We selected four commercial activated carbon and sixteen gamma irradiated-modified carbons derived from these and triiodinated contrast medium diatrizoate (DTZ) was chosen as the contaminant model. The different advanced oxidation/reduction processes studied were improved through the addition of activated carbon in the UV light and gamma radiating processes. We studied the interaction of radicals generated by oxidizing pathway (UV/activated carbon process) and spices formed by reductive process (gamma radiation/activated carbon process) with different activated carbons. The individual study of both processes, UV/activated carbon process and gamma irradiated/activated carbon process, showed that activated carbon played a decisive role in the speed of degradation of DTZ and that activated carbon did not behave as an inert material as others authors defend. In both systems, we showed that activated carbon was capable of stabilizing the radicals generated, through their conjugate surface groups or graphene sheets, which improved the removal of the DTZ, provided that there were adsorbent-adsorbate electrostatic interactions. If there were no such interactions, or these were impeded, the synergistic effect due to the action of the activated carbon did not occur. These results suggested that activated carbon had catalytic activity under different energy sources. Based on these results, we propose that activated carbon stabilizes the radicals on its surface, increasing radicals in the medium and favouring the elimination of pollutants. This effect is independent of the textural properties but not the chemical properties of the activated carbon, observing a higher effect for carbons with a higher surface content of oxygen, specifically quinone groups. Finally, we want highlight that the effect catalytic of activated carbon requires adsorbent-adsorbate electrostatic interactions.

Keywords: UV radiation; activated carbon; band gap; photocatalysis; sodium diatrizoate; radiolysis.

Abbreviation: Advanced Oxidation/Reduction Processes (AORPs), activated carbon (AC), sodium diatrizoate (DTZ), Ceca AC-40 (C), Merck (M), Sorbo-Norit (S), Witco (W), X-ray photoelectron spectroscopy (XPS), solvated electrons (e_{aq}^-), hydrogen radicals ($H^\bullet$), hydroxyl radicals ($OH^\bullet$), pH of point of zero charge (pHPZC), initial pH (pHinitial), final pH (pHfinal), surface area (SBET), Brunauer-Emmett-Teller (BET) model, total pore volume (VT), pore diameter (Dp), micropore volume (V0(N2)), and external surface volume (SExt), ultramicropore volume (V0 (CO2)), diffuse reflectance spectra (DRS), high performance liquid chromatography (HPLC), UV/activated carbon process (UV/AC), band gap (Eg).

Introduction

Advanced Oxidation Processes (AOPs) or Advanced Oxidation/Reduction Processes (AORPs) appear to be a promising technology for removing organic compounds that are resistant to conventional biological treatments. The activated carbon has the capacity to improve AOPs or AORPs in which is present. Adsorption on activated carbons (ACs) has been proposed as a method to remove this type of recalcitrant pollutant from effluents. The utilization of AC to eliminate organic and inorganic compounds from water is currently considered one of the best options available for the tertiary treatment of urban wastewater treatment plant effluents. AC can remove a large amount of pollutants of different types[1-4] due to the physicochemical properties of its surface[5]. These properties can be modified by using different activation methods, allowing the preparation of carbons to be tailored for specific objectives[6-9]. This versatility in their application is widened by their combination with other physical and chemical processes, such as AOPs, or by their application in catalysis, yielding innumerable possibilities for the treatment of all kinds of pollutants[10-14]. The utilization of ACs to enhance conventional treatment systems is therefore of great interest.

**Corresponding author: Jesús J. López-Peñalver*
E-mail address: jjpenalver@ugr.es
DOI: http://dx.doi.org/10.13171/mjc.4.2.2015.04.01.16.40/*Lopez-Penalver*

Photocatalytic processes are well known advances oxidation processes, which require the use of luminous radiation capable of producing electronic activation of the catalyst. Various materials have been used as photocatalysts but documented drawbacks of utilizing these materials include: the difficulty of their removal from the treated effluent, the necessity to their recovery and reutilization, the reduced percentage absorption of the solar spectrum, and the high level of recombination of electron-hole pairs. Recent investigation shave centered on photocatalysis processes that reduce these disadvantages. The immobilization of these photocatalysts in porous carbon materials is a research line of special interest, as reflected by the exponential increase in the number of publications over the past few years[15-21]. The photocatalytic process can be improved by the physical and chemical properties of activated carbons, especially their large specific surface area, which is usually attributed to the increase in contact surface area between catalyst and pollutant, favored by the action of the carbon as porous support[20,22-24]. In earlier investigations, we have reported that activated carbon has photochemical activity in the absence of conventional semiconductors, improving the photooxidation of pollutant[25].

On the other hand, the oxidizing pathway used to treat certain pollutants can be very slow, and the use of reducing radicals is more effective, including solvated electrons (e_{aq}^-) or hydrogen radicals ($H^\bullet$). Hence, the application of technologies that simultaneously generate oxidizing and reducing species, as in the case of ionizing radiations, may be of value in the treatment of pollutants resistant to conventional techniques. Thus, currently the ionzing radiation is applied to treat water contaminated with pollutants resistant to advanced oxidation processes[26-29]. However, there has been little research on the effects of the presence of catalysts, specifically AC, during the irradiation of contaminated waters. The application of AC with radiolysis may create a synergic effect that enhances the compound degradation, producing higher percentage degradation values than would be expected by adding together the effects of oxidizing radicals and reducing radicals from the radiolysis and adsorptive effect from AC. The use of AC in the presence of energy sources represents a novel procedure that could be applied in current radiolysis based effluent treatment systems and improve their effectiveness[26-29] because in the same treatment contaminants can be (i) adsorbed on AC, and/or (ii) oxidized due to the generation of hydroxyl radical ($OH^\bullet$) species, and/or (iii) reduced due to the formation of solvated electrons, increasing the benefit of the process.

Sodium diatrizoate has been selected as a contaminant model to evaluate the effect of the proposed processes in this study. DTZ is an iodate contrast media used in hospitals, it is highly polar, stable, and chemically inert and is eliminated unmetabolized after its administration. Thereby, this compound has been detected in urban wastewaters, surface waters, and ground waters[30-34]. Diatrizoate is not mineralized in the environment[35,36] but can degrade, resulting in stable by-products that are potentially more harmful than the original compound[36-38]. Even it was shown the high resistant from DTZ to physicochemical process as the ozonation method and ozone joint with UV lamp and hydrogen peroxide, in which DTZ degradations were 14% and 36% respectively[39,40].

With this background, the main aims of this study were to analyze the effect of adding different ACs on the radiolytic process and to identify the origin of the photocatalytic behavior of ACs in the presence of UV light. For this purpose, we selected four commercial carbons and sixteen gamma-irradiated activated carbons derived from these[41]. The specific objectives were to study: (i) the adsorption kinetics of DTZ on the commercial activated carbons and the gamma-radiated carbons under different experimental conditions; (ii) the DTZ degradation kinetics by direct photolysis with low-pressure UV radiation; (iii) the DTZ photodegradation in the presence of activated carbons; and (iv) the mechanism under-lying DTZ degradation with UV light in the presence of activated carbon, determining the role of the physical and chemical properties of the activated carbon in this process; (v) the kinetics of the radiolysis in the presence of different types of AC; (vi) the mechanisms involved in DTZ removal with the combined use of AC and radiolysis, and (vii) the influence of the physical and chemical characteristics of the ACs on the outcomes of this combined treatment.

Experimental Section

Reagents

All chemical products used (sodium diatrizoate, phosphoric acid, sodium chloride, potassium bromide, sodium nitrate, sodium carbonate, acetonitrile, formic acid) were high-purity analytical grade and supplied by Sigma-Aldrich. All solutions were prepared with ultra-pure water obtained using Milli-Q® equipment (Millipore). Four commercial activated carbons were used: Ceca AC-40 (C), Merck (M), Sorbo-Norit (S), and Witco (W). Activated carbon particle had a size less than 0.25 mm.

Determination of sodium diatrizoate in aqueous solution

DTZ concentrations in solution were determined by high performance liquid chromatography (HPLC) in inverse phase using a chromatograph (Thermo-Fisher) equipped with UV-vis detector and an autosampler with capacity for 120 vials. The chromatographic column was a Nova-Pak® C18 (4 μm particle size; 3.9×150 mm). The mobile phase was 80% of water solution (1% phosphoric acid) and 20% ultrapure water, in isocratic mode, with 2.0 mL min^{-1} flow; the detector wavelength was set at 254 nm and injection volume was 100 μL.

Photolysis of sodium diatrizoate

DTZ degradation experiments using UV radiation and UV/activated carbon processes (UV/AC) were conducted in a photoreactor (inner diameter of 13 cm × height of 45 cm) with walls of stainless steel. The photoreactor is equipped with a sample holder with a capacity for 6 quartz tubes (wall-width of 3 mm, inner diameter of 15 mm, height of 300-mm) that have a 92% transmittance for a wavelength of 254 nm. A low-pressure mercury lamp (Hg 253.70 nm) Heraeus Noblelight, model TNN 15/32 (15 W), is placed in the center of the sample holder to ensure uniform irradiation of the six quartz tubes. The photoreactor was filled with ultrapure water that surrounded the sample holder and mercury lamp and was maintained in continuous recirculation at a constant temperature (298.0±0.2 K) using a Frigiterm ultra thermostat. The photoreactor was equipped with a magnetic agitation system for maintaining the solutions within the quartz tubes under constant agitation.

For the study of direct DTZ photolysis, three 25 mg L^{-1} DTZ solutions were prepared at pH 2, 6.5, and 12, and 30 mL of the respective solutions were placed in the quartz tubes in the photoreactor. These solutions were maintained under constant agitation during the entire experiment at a temperature of 298 K and with the application of UV light at 253.70 nm wavelength. Samples were drawn from each solution at regular time intervals for subsequent measurement of the DTZ concentration.

Diatrizoate degradation by the UV/activated carbon system

Experimental data for DTZ photodegradation with activated carbon were obtained by the UV irradiation (253.70 nm) of 25 mg L^{-1} solutions of DTZ in the presence of 5 mg activated carbon at pH 6.5 and 298 K under constant agitation. Samples were drawn at regular time intervals to follow DTZ degradation kinetics. Samples were immediately filtered by Millipore disk filters (0.45 μm) to remove the activated carbon.

Gamma irradiation source

Irradiation experiments were conducted using a JL Shepherd Mark 1 gamma irradiator (model 30J) in the Experimental Radiology Unit of the Scientific Instrumentation Center of the University of Granada (Spain). The equipment includes four 137 Cs radioactive sources with a total combined activity of 3.70×10^{13} Bq (1000 Ci). The irradiation chamber has a useful volume of 8.25 L and is equipped with a rotation system that guarantees uniform dose application throughout the irradiation volume. The apparatus has three irradiation positions for different dose rates: position 1, 3.83 Gy min^{-1}; position 2, 1.66 Gy min^{-1}; and position 3: 1.06 Gy min^{-1}.

Gamma-irradiated activated carbons

All activated carbons used were texturally and chemically characterized as described in detail elsewhere[41]. ACs characteristics are given in Tables S1 (Textural characteristics) and S2 (Chemical characteristics) in the supplementary data. Table 1 shows the designation of different activated carbon used

.

Table 1. Designations of the activated carbon samples

Ceca series	C	Pristine activated carbon Ceca
	C-$H^{\bullet}$	Activated carbon irradiated in the presence of $H^{\bullet}$
	C- e^{-}_{aq}	Activated carbon irradiated in the presence of e^{-}_{aq}
	C-$OH^{\bullet}$	Activated carbon irradiated in the presence of $OH^{\bullet}$
	C-0	Activated carbon irradiated in the presence of all radicals
Merck series	M	Pristine activated carbon Merck
	M-$H^{\bullet}$	Activated carbon irradiated in the presence of $H^{\bullet}$
	M- e^{-}_{aq}	Activated carbon irradiated in the presence of e^{-}_{aq}
	M-$OH^{\bullet}$	Activated carbon irradiated in the presence of $OH^{\bullet}$
	M-0	Activated carbon irradiated in the presence of all radicals
Sorbo series	S	Pristine activated carbon Sorbo
	S-$H^{\bullet}$	Activated carbon irradiated in the presence of $H^{\bullet}$
	S- e^{-}_{aq}	Activated carbon irradiated in the presence of e^{-}_{aq}
	S-$OH^{\bullet}$	Activated carbon irradiated in the presence of $OH^{\bullet}$
	S-0	Activated carbon irradiated in the presence of all radicals
Witco series	W	Pristine activated carbon Witco
	W-$H^{\bullet}$	Activated carbon irradiated in the presence of $H^{\bullet}$
	W- e^{-}_{aq}	Activated carbon irradiated in the presence of e^{-}_{aq}
	W-$OH^{\bullet}$	Activated carbon irradiated in the presence of $OH^{\bullet}$
	W-0	Activated carbon irradiated in the presence of all radicals

Sodium diatrizoate degradation kinetics by radiolysis

DTZ degradation kinetics with gamma irradiation were obtained by irradiating 1000 mg L^{-1} DTZ at 298 K and pH 6.5 drawing samples at different doses (25, 50, 100, 200, 400, 600 Gy) and the DTZ concentration was determined for these doses. The dose rate was 1.66 Gy min^{-1}.

DTZ samples were irradiated at room temperature (298 ± 2 K) in 2 mL vials sealed with screw tops to avoid the entry of air. Before the irradiation, nitrogen was bubbled through the samples to avoid the presence of dissolved oxygen in the medium.

Sodium diatrizoate radiolysis in the presence of activated carbon

The experimental conditions for DTZ radiolysis in the presence of AC were the same as those for the adsorption and radiolysis experiments in the absence of AC, irradiating 1000 mg L^{-1} DTZ at 298 K and pH 6.5, in the presence of 0.06 g AC and drawing samples after different doses (25, 50, 100, 200, 400, and 600 Gy). All samples were immediately filtered (Millipore filters, 0.45 μm) to remove the AC before determining DTZ concentration of each sample.

Study of the radicals responsible for sodium diatrizoate degradation during radiolysis

Gamma irradiation breaks the water molecule, forming various highly reactive radical species, both oxidizing ($OH^{\bullet}$) and reducing ($H^{\bullet}$, e^-_{aq}). The influence of these radicals generated in radiolysis on DTZ degradation was studied by irradiating 1000 mg L^{-1} DTZ solutions in the presence of 0.06 g AC, using carbons S and C as models. For this purpose, we added the corresponding salts (NaCl, KBr, $NaNO_3$) to reach concentrations in the reaction medium of 1000 mg L^{-1} of: (i) Cl^- anion at pH = 1.0, when $H^{\bullet}$ is the predominant radical species in the medium because this anion acts as $OH^{\bullet}$ radical scavenger (Reaction 2-9), and at pH 1.0, when the reaction of e^-_{aq} with H^+ is favored (Reaction 10)[42,43]; (ii) anion Br^- at pH = 7.5, with this ion acting as $HO^{\bullet}$ radical scavenger (Reactions 11-14)[44-46] and the pH favoring the reaction of $H^{\bullet}$ radicals with the hydroxyl anions present (Reaction 15), resulting in the predominance of solvated electrons in the medium; and (iii) anion NO_3^- at pH=12.5, when the $OH^{\bullet}$ radical is the predominant species in the medium, because the NO_3^- anion acts as $H^{\bullet}$ and e^-_{aq} scavenger (Reactions 16, 17)[43,46,47]. All samples were bubbled with nitrogen to prevent the presence of dissolved oxygen, and the vials were sealed to prevent the entry of air.

The influence of the presence of the above anions on DTZ irradiation in the absence of ACs and on DTZ adsorption on activated carbons was assessed by preparing samples under the same conditions as for the radiolysis in the presence of AC. Samples were again drawn at the times corresponding to the doses of 25, 50, 100, 200, 400, and 600 Gy, and all samples containing AC were immediately filtered (Millipore filter, 0.45 μm). The DTZ concentration of all these samples were determined.

Sodium diatrizoate adsorption kinetics on activated carbons

For comparison with experiments in which gamma radiation is applied, the experimental data of DTZ adsorption on the ACs were obtained by placing 0.06 g of AC in contact with 5 mL of 1000 mg L^{-1} DTZ solution at 298 K and pH 6.5. DTZ adsorption on the different ACs was determined by conducting adsorption experiments under the same conditions as those for the irradiations. The total experimentation time corresponded to the total dose applied in radiolysis experiments at 600 Gy, i.e., 361.44 min. During this period of time, seven samples were drawn for subsequent measurement of DTZ concentration, corresponding to doses of 25 Gy (15.06 min), 50 Gy (30.12 min), 100 Gy (60.24 min), 200 Gy (120.48 min), 400 Gy (240.96 min), and 600 Gy (361.44 min). The samples were immediately filtered with Millipore filters (0.45 μm) to remove the AC present.

On the other hand, in the case of experiments with UV radiation, the experimental data for DTZ adsorption kinetics on activated carbons were obtained by placing 5 mg of activated carbon in contact with 30 mL of 25 mg L^{-1} DTZ solution at 298 K and pH 6.5. Samples were drawn at regular time intervals to determine the DTZ concentration for calculation of the amount adsorbed. The experimentation conditions for the adsorption process were the same as for UV degradation in the presence of activated carbon.

Results and Discussion

Diatrizoate degradation with UV light in the presence of activated carbon

We investigated the degradation of DTZ when activated carbon was present during the photolytic process (UV/AC). Figure 1 depicts DTZ removal by UV radiation and by the simultaneous use of UV radiation and activated carbons C, S, M, or W. It is observed that the removal rate is markedly increased by the presence of activated carbon.

Based on the degradation kinetics obtained, we calculated the values of the reaction rate constants in Table 2. The values of these constants confirm the increase in reaction rate observed in the degradation kinetics. This may be attributable to the contribution to the overall removal process of DTZ adsorption on the activated carbons. For this reason, we obtained the DTZ adsorption kinetics on all of the activated carbon samples. The results in Table 2 show that carbons on W series have the lowest adsorptive contribution to the global removal process, but these activated carbons produce the greatest increase in DTZ removal by the UV/AC system.

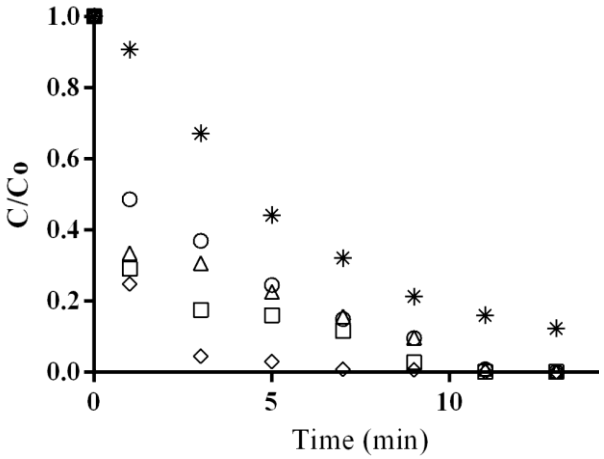

Figure 1. DTZ degradation by direct photolysis (✳) and by the UV/AC system with activated carbons C (○), M (△), S (□), or W (◇). $[DTZ]_0$=25 mg L^{-1}; pH=6.5; T=298 K.

These results indicate that DTZ adsorption on activated carbon is not the sole cause for the increase in DTZ removal in the UV/AC system and that the activated carbon must make other types of contribution to the overall removal process.

The role of activated carbon in DTZ removal process by UV/AC was further explored by determining the percentage removal (designated "synergic effect") of the carbons, which was calculated by subtracting the adsorptive and photolytic contributions from the global removal percentage in the UV/AC system (Eq. (1)). Results are listed in Table 2.

$$\% S_{UV/AC} = \% D_{UV/AC} - \%D_{UV} - \%A_{AC} \quad \textbf{(1)}$$

where $\%S_{UV/AC}$ is the percentage DTZ removal due to the synergic effect produced by the presence of activated carbon during exposure to UV radiation, $\%D_{UV/AC}$ is the total percentage DTZ removal in the photocatalytic process UV/AC, $\%D_{UV}$ is the percentage DTZ degradation by direct photolysis, and $\%A_{AC}$ is the percentage DTZ removal by adsorption on the activated carbon.

Among the different commercial activated carbons used, the results in Table 2 show that carbon S made the highest adsorptive contribution to the global removal process and carbon W the lowest. However, we highlight that carbon W exerts the greatest synergic effect on DTZ removal by the UV/AC system, with a synergic contribution of >53% after the first minute of treatment.

Table 2. Removal fractions and reaction rate constants for DTZ removal by UV/AC. $[DTZ]_0$=25 mg L^{-1}; pH=6.5; T=298 K.

Exp. Num.	Activated carbon	K_{OB} (15 min) (min^{-1})	% UV degradation (1 min)	% Removal by adsorption (1 min)	% Removal by UV/AC (1 min)	% Synergic removal (1 min)
1	C	0.47 ± 0.01	9.29	14.20	51.50	28.01
2	C-H$^{\bullet}$	0.75 ± 0.04	9.29	11.70	49.79	28.80
3	C- e_{aq}^-	0.69 ± 0.03	9.29	11.60	44.61	23.72
4	C-OH$^{\bullet}$	1.05 ± 0.05	9.29	17.00	53.99	27.70
5	C-0	2.05 ± 0.00	9.29	12.90	87.09	64.90
6	M	0.53 ± 0.04	9.29	18.70	66.60	38.61
7	M-H$^{\bullet}$	1.06 ± 0.02	9.29	30.40	65.38	25.69
8	M- e_{aq}^-	1.05 ± 0.04	9.29	0.86	65.04	54.89
9	M-OH$^{\bullet}$	0.93 ± 0.05	9.29	17.00	62.36	36.07
10	M-0	0.69 ± 0.04	9.29	12.40	53.05	31.36
11	S	0.59 ± 0.03	9.29	28.80	71.00	32.91
12	S-H$^{\bullet}$	0.42 ± 0.05	9.29	8.49	45.00	27.22
13	S- e_{aq}^-	0.28 ± 0.02	9.29	9.07	32.49	14.13
14	S-OH$^{\bullet}$	1.03 ± 0.04	9.29	14.80	64.10	39.91
15	S-0	1.07 ± 0.02	9.29	7.67	47.00	30.04
16	W	1.42 ± 0.04	9.29	12.80	75.20	53.11
17	W-H$^{\bullet}$	1.02 ± 0.04	9.29	1.04	69.47	59.14
18	W- e_{aq}^-	5.06 ± 0.06	9.29	1.02	100	89.69
19	W-OH$^{\bullet}$	5.26 ± 0.06	9.29	1.67	92.81	81.85
20	W-0	0.99 ± 0.01	9.29	8.23	62.87	45.35

Figure 2 depicts the time course of the synergic contribution to the overall DTZ removal by the UV/AC system for the four original activated carbons. The results obtained indicate that, regardless of the activated carbon used, the synergic contribution decreases with longer treatment time

.

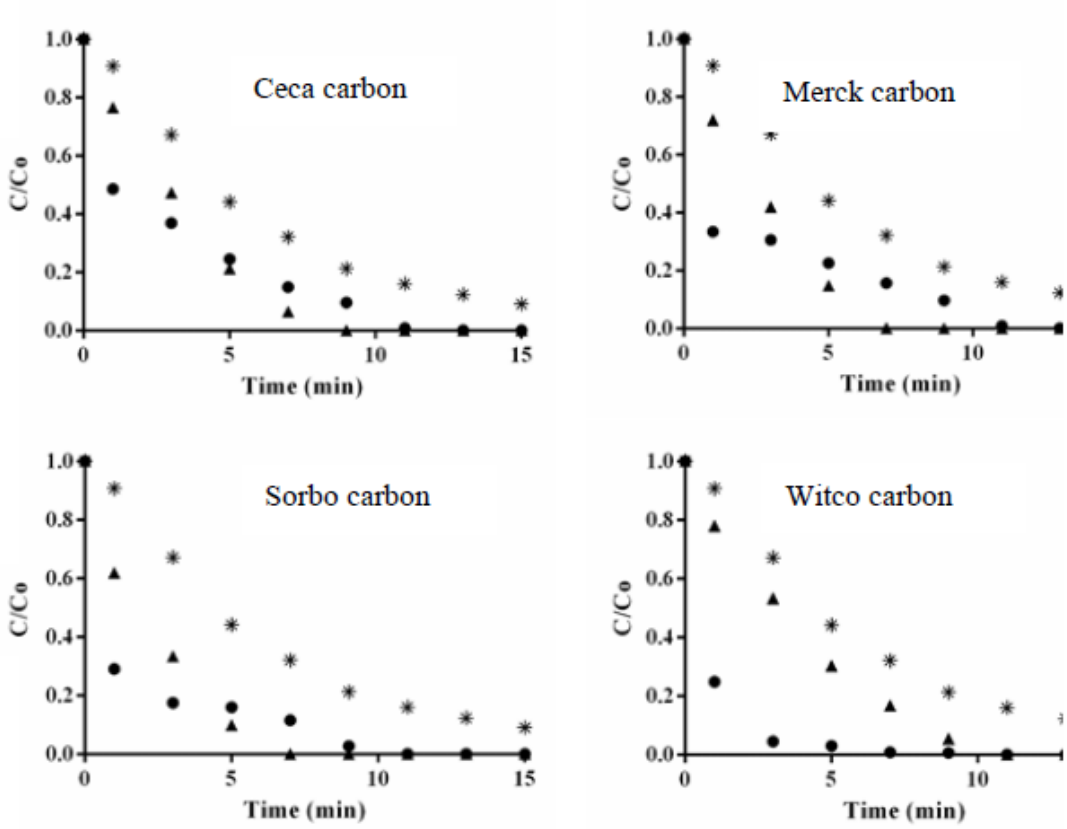

Figure 2. DTZ removal by the UV/AC system. (✳), Direct photolysis; (●), UV/AC; (▲), V + adsorption. $[DTZ]_0$=25 mg L^{-1}; pH=6.5; T=298 K.

The influence of the surface chemistry of activated carbon on DTZ degradation by the UV/AC system was studied using carbons that had undergone different gamma irradiation treatments. These treatments modified the surface chemistry of the carbons (Tables S2 - S5 in supplementary data) but not their textural characteristics (Table S1, in supplementary data). Thus, we obtained carbons treated with reducing agents (solvated electrons, e_{aq}^-, and hydrogen atoms, H•) and carbons treated with oxidizing agents (OH• radicals). The nomenclature of the resulting carbons and their chemical and textural characteristics are given in Table 1 and Tables S1 - S5 (supplementary data).

Figure 3 depicts the time course of the relative DTZ concentration during UV/AC treatment of the four series of activated carbons. We shall first discuss the results of carbon W (Fig. 3D), the activated carbon showing the greatest synergic activity. According to the results, the carbons producing the greatest increase in DTZ removal are W-e_{aq}^- and W-OH•. These results appear to indicate that, regardless of the treatment applied (oxidizing or reducing agents) irradiation of the activated carbon increases its synergic activity. The chemical properties of the treated carbons[41] (Tables S2 - S5, in supplementary data) show that both treatments increase the percentage of Ph-OH, C-O (ester/anhydride) groups in comparison to the original carbon. The textural and chemical properties of the activated carbons used show no clear relationship with their synergic contribution. However, the synergic activity of the activated carbon is more greatly enhanced by the samples with higher percentages of surface oxygen and, among these, the samples with higher percentages of carbon atoms with sp^2 hybridization.

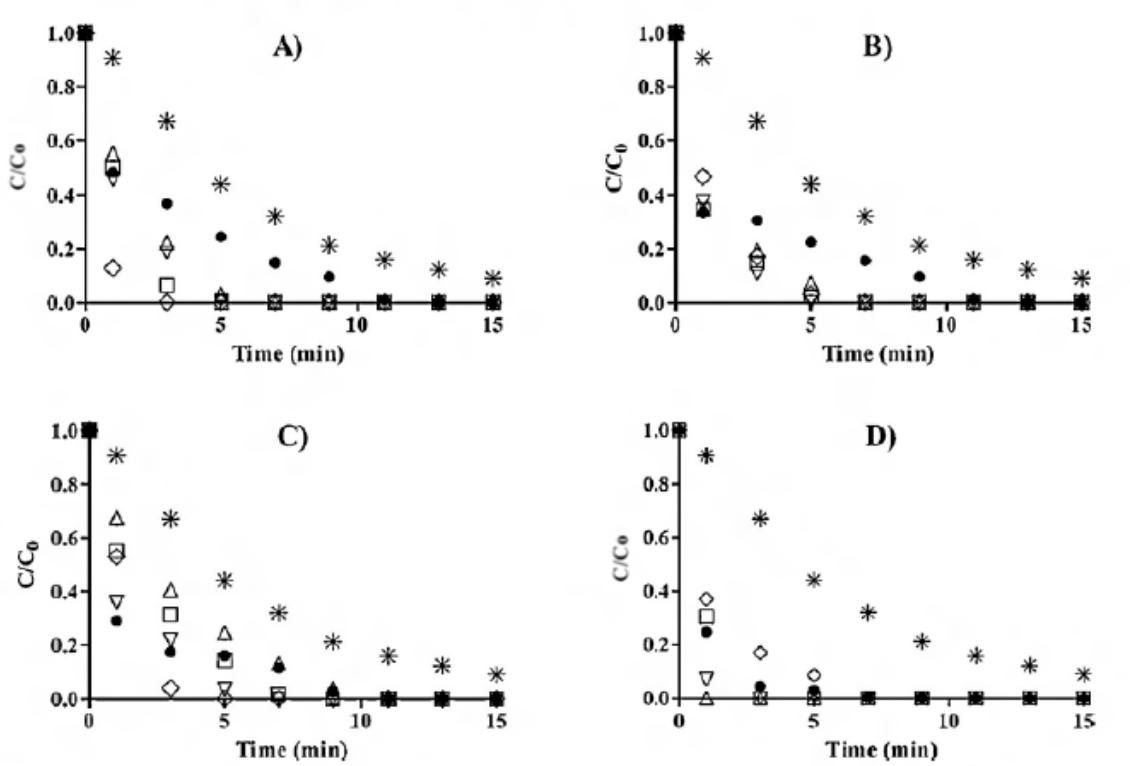

Figure 3. Time course of DTZ degradation fraction with the UV/AC system. (∗), Direct photolysis; (●), UV/AC; (□), UV/AC-H•; (△), UV/AC-e_{aq}^-; (▽), UV/AC-OH•; (◇), UV/CA-0. (A) Carbon C; (B) Carbon M; (C) Carbon S; (D) Carbon W. $[DTZ]_0$=25 mg L^{-1} ; pH=6.5; T=298 K.

In order to dig deep into the activated carbon characteristics affecting its photocatalytic activity, we have determined the band gap (Eg) of the activated carbons[41]. Determination of the activated carbon band gap demonstrated that these materials behave as semiconductor materials and therefore as photoactive materials in the presence of UV light, because all Eg values are <4 eV (Table 3). In general, the gamma radiation treatment reduces the band gap energy of the materials and, within the same series of activated carbons, lower Eg values correspond to higher DTZ degradation values

.

Table 3. Band gap values (Eg) of the activated carbons, calculated according to the Kubelka-Munk method.

Processing	Serie C E_g ± SD (eV)	Serie M E_g ± SD (eV)	Serie S E_g ± SD (eV)	Serie W E_g ± SD (eV)
AC [a]	3.65 ± 0.06	3.50 ± 0.04	3.58 ± 0.04	3.68 ± 0.04
AC-0 [b]	3.04 ± 0.04	3.33 ± 0.04	2.98 ± 0.04	3.23 ± 0.04
AC-H• [c]	3.36 ± 0.04	3.13 ± 0.04	3.63 ± 0.04	3.35 ± 0.04
AC-e^-_{aq} [d]	3.14 ± 0.04	3.20 ± 0.04	3.16 ± 0.04	3.15 ± 0.04
AC-OH• [e]	3.00 ± 0.04	3.23 ± 0.04	2.92 ± 0.04	3.10 ± 0.04

[a]AC pristine; [b]AC irradiated in ultrapure water; [c]AC irradiated in ultrapure water, pH=1.0 y $[Cl^-]$=1000 mg L^{-1}; [d]AC irradiated in ultrapure water, pH=7.5 y $[Br^-]$=1000 mg L^{-1}; [e]AC irradiated in ultrapure water, pH=12.5 y $[NO_3^-]$=1000 mg L^{-1}.

Our results showed that there was a positive correlation between the sp^3/sp^2 ratio and the Eg value ($P< 0.05$, r=0.4823, Table S6 in supplementary data), revealing that an increase in sp^2 hybridization was associated with a decrease in Eg value, because a larger fraction of sp^2 C atoms increases extensive π conjugation and reduces band gap[48].

The ultraviolet radiation absorption in carbon materials is caused by electronic transitions between the bonding and antibonding π orbitals, since the π- π* transitions are located in the range between 180 and 260 nm. On the other hand, structural changes are correlated with a different optical behavior of these materials. Thus, the greater the content of sp^2 hybridized carbon the greater is the UV peak position in wavelength and therefore the photocatalytic activity of the carbon is favored.

When an incident photon has energy greater than the band gap it is absorbed and created an electron-hole pair. The photogenerated electrons would spread throughout the graphene layers and reach molecules of the absorbed pollutants and/or oxygen molecules.

The electrons would reduce the adsorbed O_2 to form superoxide radicals ($O_2^{\bullet-}$), which can react with the water molecule and trigger the formation of oxidizing radical species (Reactions 2-4) that will interact with the contaminants, contributing to its degradation[49].

$$e_{CB}^- + O_2 \rightarrow O_2^{\bullet-} \quad \textbf{(2)}$$

$$O_2^{\bullet-} + H_2O \rightarrow HO_2^{\bullet} + HO^- \quad (3)$$

$$2HO_2^{\bullet} \rightarrow O_2 + H_2O_2 \rightarrow O_2 + 2OH^{\bullet} \quad (4)$$

The positive holes are directly responsible for the generation of hydroxyl radicals by interaction with water molecules (Reaction 5).

$$h_{BV}^+ + H_2O \rightarrow OH^{\bullet} + H^+ \quad \textbf{(5)}$$

Based on these backgrounds, we propose that the photons from UV light would fall on the activated carbons and generate electron-hole pairs through their irradiation with a sufficient amount of energy to promote electrons from the valence band to the conduction band. The photogenerated electrons would spread throughout the graphene layers and reach molecules of the absorbed DTZ and oxygen molecules. The electrons reduce the adsorbed O_2 to form superoxide radicals ($O_2^{\bullet-}$), which can react with the water molecule and trigger the formation of oxidizing radical species[49] that will interact with the pollutants, contributing to its degradation. Additionally, the presence of adsorbed oxygen avoids recombination of the electron with the positive hole (Reactions 2-4), allowing interaction between the water molecule and the free hole and increasing the effectiveness of the photocatalytic process. The positive holes are directly responsible for the generation of hydroxyl radicals by interaction with OH^- groups of the carbon surface and by capture of water molecules. All this would explain the DTZ photodegradation would be encouraged in the presence of activated carbon.

Finally, we decided to study the role of activated carbon in the stabilization of the radicals formed, and for that we irradiated DTZ samples in the presence of activated carbon.

(2)

Diatrizoate degradation by gamma radiation in the presence of activated carbon **(3)**

(4)

DTZ radiolysis in the presence of AC is a complex process. The degradation of DTZ by the radical species generated through the interaction of gamma radiation with the water molecule is simultaneous with the adsorption of DTZ on the AC in the medium. The influences of DTZ adsorption and radiolysis was quantified by obtaining the adsorption and radiolysis kinetics separately under the same experimental conditions as those used to obtain DTZ degradation kinetics in the presence of AC.

Figure 4 depicts the removal kinetics obtained when using the carbons, showing that the final percentage DTZ removal at a dose of 600 Gy is much higher in the presence of the ACs than in their absence. The difference between the effect of radiolysis in the presence of AC and the sum of the effects of DTZ radiolysis without AC and adsorption was more marked in the case of carbons C and M. The synergic effect was lower when the DTZ adsorption rate was higher, as in the case of carbon S.

However, account must be taken of the adsorption of DTZ on the AC to assess whether the improvement observed is merely the sum of the effects of AC adsorption and gamma radiation or whether the presence of AC enhances the degradation, revealing a synergic effect of their combined use.

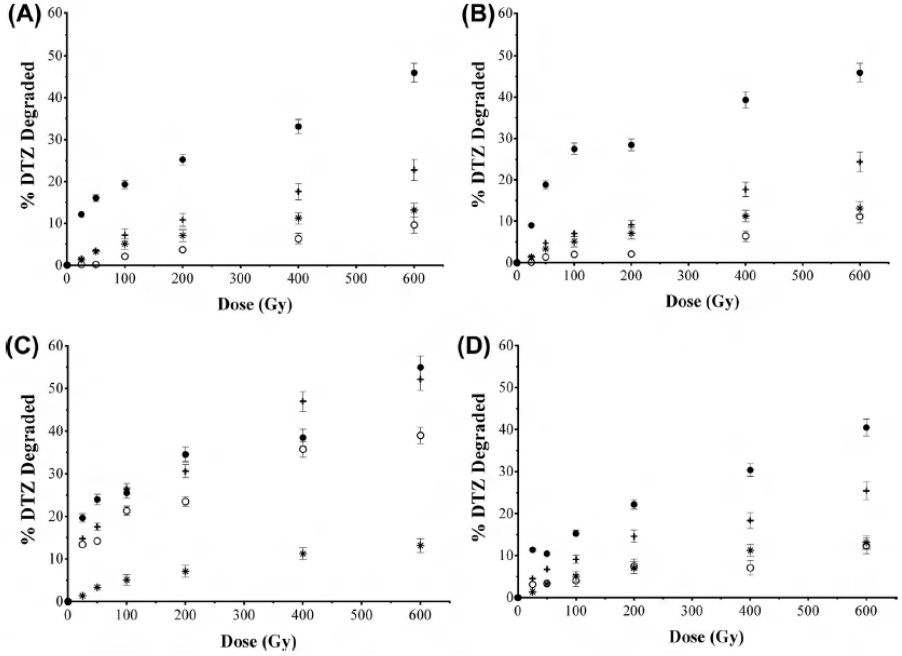

Figure 4. Percentage DTZ removal with four systems: (∗) radiolysis without AC; (●) radiolysis in the presence of AC; (○) DTZ adsorption on AC; and (+) theoretical sum effect of adsorption plus radiolysis.

(A), Carbon C series; (B), carbon M series; (C), carbon S series; (D), carbon W series. [DTZ_0]=1000 mg L^{-1}. Amount of AC=0.06 g. T=298 K. pH=6.5. Dose Rate=1.66 Gy min^{-1}.

Comparison of the results (Figure 4) with the chemical and textural characteristics of the ACs (Tables S1 - S5 in supplementary data) showed that the synergic effect was not influenced by their textural characteristics. Therefore, the ability of the ACs to enhance radiolytic DTZ degradation by the use of gamma radiation may be related to their chemical properties. In order to understand this behavior, it should be taken into account that the gamma radiation interacts with both the AC and the water molecule. Given that carbon has a low atomic number and the radiation has an energy of 0.6617 MeV, the Compton effect would be predominant interaction of gamma radiation with matter in the case of ACs[50]. The main interaction mechanism in the Compton effect is ionization, by which incident photons can interact with the orbital electrons of surface atoms and produce positive ions and free electrons. Hence, the carbon atoms on the surface would contribute to increasing the free electrons in the medium, favoring DTZ degradation (reduction pathway), which would explain the synergic effect observed for the four ACs. Moreover, as reported by Boehm[49], the chemisorbed oxygen on the four carbons (Table S1, supplementary data) can scavenge electrons and give rise to the formation of the superoxide anion. This anion can directly interact with DTZ, form radicals by Reaction 6, or establish the balance of Reaction 7 to yield Reactions 8 and 9, forming H_2O_2[51,52].

$$O_2^{\bullet-} + H_3O^+ \longrightarrow OH^\bullet + H_2O + {}^1/_2\ O_2 \qquad k = 4.5\times10^{10}\ M^{-1}\ s^{-1} \qquad \textbf{(6)}$$

$$H^+ + O_2^{\bullet-} \leftrightarrows HO_2^\bullet \qquad k_{eq} = 1.5\times10^{-5}\ M^{-1}\ s^{-1} \qquad \textbf{(7)}$$

$$HO_2^\bullet + O_2^{\bullet-} \longrightarrow HO_2^- + O_2 \qquad k = 8.9\times10^{7}\ M^{-1}\ s^{-1} \qquad \textbf{(8)}$$

$$HO_2^\bullet + HO_2^\bullet \longrightarrow H_2O_2 + O_2 \qquad k = 2.0\times10^{6}\ M^{-1}\ s^{-1} \qquad \textbf{(9)}$$

All of the above would contribute to increasing DTZ degradation by favoring new oxidizing species in the medium. In addition, incident gamma radiation interacts with the water molecule, giving rise to the processes described in Reactions 10-14[53,54]

$$H_2O \xrightarrow{\text{Radiation } \gamma} H_2O^{\bullet+} + e^- \qquad \textbf{(10)}$$

$$H_2O \xrightarrow{\text{Radiation } \gamma} H_2O^* \qquad \textbf{(11)}$$

$$H_2O^{\bullet+} \longrightarrow OH^\bullet + H^+ \qquad \textbf{(12)}$$

$$e^- + nH_2O \longrightarrow e_{aq}^- \qquad \textbf{(13)}$$

$$H_2O^* \longrightarrow OH^\bullet + H^\bullet \qquad \textbf{(14)}$$

Radiolysis radicals are formed by the above reactions, and these can interact with both the DTZ and AC in the medium, also giving rise to radical recombination reactions (Reactions 15-18)[43].

$$OH^\bullet + H^\bullet \longrightarrow H_2O \qquad k = 7.0\times10^{9}\ M^{-1}\ s^{-1} \qquad \textbf{(15)}$$

$$H^\bullet + H^\bullet \longrightarrow H_2 \qquad k = 7.8\times10^{9}\ M^{-1}\ s^{-1} \qquad \textbf{(16)}$$

$$e_{aq}^- + H^\bullet + H_2O \longrightarrow H_2 + HO^- \qquad k = 2.5\times10^{10}\ M^{-1}\ s^{-1} \qquad \textbf{(17)}$$

$$OH^\bullet + e_{aq}^- \longrightarrow HO^- \qquad k = 3.0\times10^{10}\ M^{-1}\ s^{-1} \qquad \textbf{(18)}$$

Voudrias et al.[55] used electron spin resonance to demonstrate that oxygenated groups on the AC, especially quinone groups, can stabilize radicals on its surface, as well as the conjugated aromatic rings system. It is possible that interaction between the radicals formed during radiolysis and the carbon surface gives rise to areas with high reactivity, due to radicals stabilized by the quinone groups on the AC surface. This mechanism would be more influential with greater quinone content, explaining why the best results were obtained with carbon S (Figure 4C).

The influence of each species formed during water radiolysis was analysed to explore further the mechanisms underlying the synergic activity of AC in DTZ degradation, conducting experiments in which one of the three radiolysis-induced species ($OH^\bullet$, $H^\bullet$, or e^-_{aq}) was predominant. Table 4 exhibits the data for DTZ radiolysis in the absence and presence of AC and in the presence of scavengers and shows the adsorption and radiolysis degradation values in the presence of AC. The values obtained for k_{ob} in the presence of anion Cl^-, both for carbons C and S, indicate the absence of a synergic effect under these experimental conditions (Table 4, experiments 21-25), given that the radiolysis, k_{Rad}, and adsorption, k_{Ad}, values were higher than the k_{ob} value. This behavior can be explained by the positive charge of the carbon surface at the study pH (pH=1.0), because solution pH < pH_{PZC} (Table S2, supplementary data), whereas the DTZ has no charge (Figure 5). In this situation, the percentage DTZ adsorption is the lowest among the three experimental conditions studied, due to a possible screening of the carbon surface charge by the Cl^- ions in the medium, reducing the interactions between the carbon surface and DTZ molecules. This mechanism would hamper the action of the AC in DTZ radiolysis. Furthermore, the k_{Rad} value is higher than the constants determined in experiments 26 and 31 (Table 4), indicating that

radiolysis is favored under these conditions because of the elevated hydrogen reaction constant with DTZ $(2.2\pm0.5)\times10^9$ $M^{-1}s^{-1}$)[56].

Table 4. Influence of the presence of scavengers on DTZ removal. $[DTZ]_0$=1000 mg L^{-1}. P_{CA}=0.06 g de CA. $[Cl^-]$=1000 mg L^{-1}, Exp.: 21-25. $[Br^-]$=1000 mg L^{-1}, Exp.: 26-30. $[NO_3^-]$=1000 mg L^{-1}, Exp. 31-35. Dose Rate=1.66 Gy min^{-1}. T=298 K.

Nº. Exp.	CA	pH	Radical	% DTZ Removal	$k_{Rad}\times10^4$ (Gy^{-1})	$k_{Ad}\times10^4$ (Gy^{-1})	$k_{ob}\times10^4$ (Gy^{-1})
21	-	1.0	$H^\bullet$	25.87	4.8±0.2	-	-
22	C	1.0	$H^\bullet$	20.32	-	3.45±0.05	-
23	C	1.0	$H^\bullet$	35.61	-	-	3.9±0.4
24	S	1.0	$H^\bullet$	20.67	-	3.1±0.3	-
25	S	1.0	$H^\bullet$	35.97	-	-	2.61±0.08
26	-	7.5	e^-_{aq}	11.55	1.15±0.03	-	-
27	C	7.5	e^-_{aq}	23.93	-	4.1±0.2	
28	C	7.5	e^-_{aq}	37.27	-	-	7.0±0.2
29	S	7.5	e^-_{aq}	33.16	-	6.1±0.3	
30	S	7.5	e^-_{aq}	49.25	-	-	9.7±0.2
31	-	12.5	$OH^\bullet$	8.51	0.87±0.03	-	-
32	C	12.5	$OH^\bullet$	16.13	-	2.94±0.07	-
33	C	12.5	$OH^\bullet$	24.28	-	-	4.1±0.3
34	S	12.5	$OH^\bullet$	26.56	-	3.76±0.08	-
35	S	12.5	$OH^\bullet$	32.46	-	-	5.1±0.4

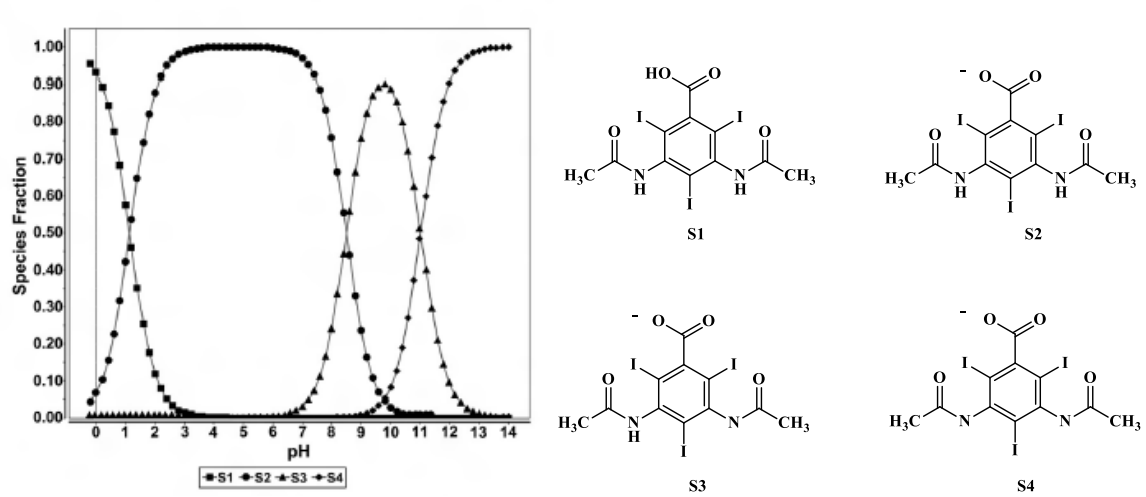

Figure 5. Molecular structure of DTZ and its species distribution as a function of solution pH.

In addition, the k_{ob} value is lower than the k_{Rad} value, suggesting that some of the $H^\bullet$ radicals formed during radiolysis interact with the AC present in the medium, forming highly reactive centers, stabilized by delocalization over the large conjugated aromatic rings system (Figure 6)[55]. The reactive centers formed would not react with DTZ because this compound cannot gain access to the carbon surface, as a result the action of chloride anions.

According to the results in Table 4, the k_{ob} value was highest when solvated electrons were the predominant species. In addition, the DTZ removal by radiolysis in the presence of AC was the highest among the three experimental conditions considered, being 49.25% for carbon S and 37.27% for carbon C. The contribution of adsorption to DTZ removal was only 23.93% for carbon C and 33.16% for carbon S, with k_{ad} values of $(4.1 \pm 0.2)\times10^{-4}$ Gy^{-1} and $(6.1 \pm 0.3)\times10^{-4}$ Gy^{-1}, respectively. This difference is attributable to their different pH_{PZC} values, given that the surface of carbon C has no charge at the study pH (pH=7.5), due to its proximity to the pH_{PZC} value,

whereas carbon S has a net positive charge and favors attractive electrostatic interactions between adsorbate and adsorbent, because DTZ has a negative charge at this pH (Figure 5). The k_{SE} values calculated for the two carbons is $(1.7 \pm 0.5)\times10^{-4}$ Gy^{-1} for carbon C and $(2.4 \pm 0.5)\times10^{-4}$ Gy^{-1} for carbon S. This difference may be attributable to the higher quinone groups content of carbon S, which can stabilize radicals on its surface, forming highly reactive centers that can degrade DTZ (Figure 7).

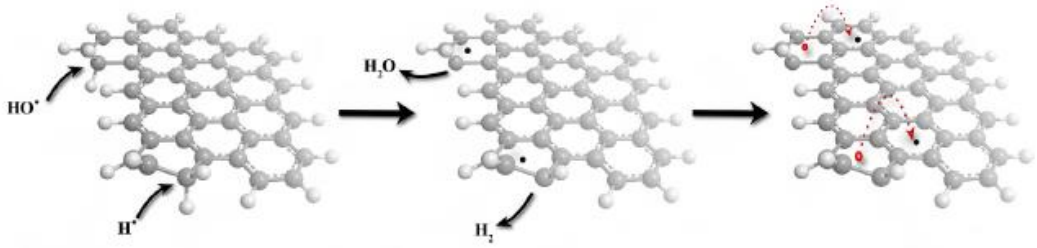

Figure 6. Stabilization of radicals by delocalization over conjugated aromatic rings system.

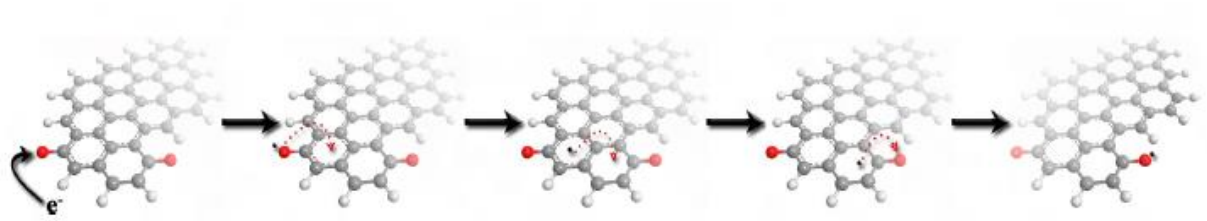

Figure 7. Stabilization of by delocalization radicals over quinone groups.

Finally, the experiments conducted in the presence of the hydroxyl radical (Table 4, experiments 31-35) showed that: (i) radiolysis is reduced in the absence of AC, degrading only 8.51% of initial concentration of DTZ and obtaining the lowest k_{Rad} value among the three experimental conditions, because the DTZ degradation reaction rate constant with the hydroxyl radical [$K_{OH\cdot}$ (DTZ) = $(5.4 \pm 0.3)\times10^{8}$ M^{-1} s^{-1}] is the lowest among the three species studied; (ii) the contribution of the adsorption process is lower, because both carbon C and S have a negative surface charge ($pH_{medium} > pH_{PZC}$), producing repulsive electrostatic interactions between adsorbent and adsorbate, given that DTZ is negatively charged at this pH (Figure 5). Hence, there is a predominance of dispersive interactions between the π electrons of the DTZ aromatic ring and the π electrons of the graphene planes of the AC (π–π interactions) in this adsorption system, as proposed by Coughlin et al.[57]; and (iii) the k_{SE} value is $(2.9 \pm 0.5)\times10^{-5}$ Gy^{-1} for carbon C and $(4.7 \pm 0.5)\times10^{-5}$ Gy^{-1} for carbon S, an order of magnitude lower than the value determined in the presence of solvated electrons; furthermore, as in the case of $H^{\bullet}$ radicals, the hydroxyl radical interacts with the AC present, which competes with the DTZ for this radical (Table 4, experiments 21-25).

Therefore, the results obtained in the presence of anions indicate that there must be a first step of electrostatic interactions between the DTZ molecules and AC surface for the synergic effect to take place. When the surface charge of the carbon hinders or impedes these interactions or when the presence of ions screen the adsorbate-adsorbent interactions, the synergic effect is reduced or even disappears.

Conclusion

The different advanced oxidation/reduction processes that have been studied shown positive results in the DTZ degradation. They were improved through the addition of AC in the UV light and gamma radiating processes.

The results of this study demonstrate that the presence of activated carbon during the DTZ photodegradation process markedly increases the removal rate, regardless of the activated carbon used. The results obtained indicate that activated carbon W exerts the greatest synergic effect on DTZ removal by the UV/AC system, with a synergic contribution >53% at one minute of treatment. Regardless of the activated carbon sample considered, its synergic activity is, in general, enhanced by the gamma radiation treatment.

The textural and chemical properties of the activated carbons used show no clear relationship with their synergic contribution. However, the synergic activity of the activated carbon is more greatly enhanced by the samples with higher percentages of surface oxygen and, among these, the samples with higher percentages of carbon atoms with sp^2 hybridization. Determination of the activated carbon band gap demonstrated that these materials behave as semiconductor materials and therefore as photoactive materials in the presence of UV radiation, because all E_g values are <4 eV.

In general, the gamma radiation treatment of activated carbons reduce the band gap energy of these materials and, within the same series of activated carbons, lower E_g values correspond to higher k_{OB} values. We indicate that the percentage of carbon atoms with sp^2 hybridization is increased in the gamma irradiation modified materials, reducing their

band gap, explaining their usually superior behavior in DTZ photodegradation.

Related to the mechanism involved in the radiolysis/AC process used, the results obtained show that the solvated electrons formed during water radiolysis may interact with the AC surface, giving rise to areas with high reactivity due to the stabilization of the radicals by the quinone groups on the surface. The influence of this mechanism would be greater with higher quinone content. Moreover, analysis of the role in DTZ removal of the radical species produced by water radiolysis shows that adsorbate-adsorbent electrostatic interactions are necessary to obtain a synergic effect on pollutant degradation.

Based on these results, an action mechanism for the removal of DTZ in the presence of activated carbon is proposed, in which the activated carbon can act as a photocatalyst, in presence of ultraviolet radiation, promoting electrons of the valence band to the conduction band and increasing the generation of $OH^{\bullet}$ radicals in the medium. Moreover, activated carbon can stabilize radicals formed on its surface, increasing the concentration of radicals, which improves the contaminant elimination process.

Acknowledgements

The authors are grateful for the financial support provided by the Junta de Andalucía (RNM7522) and the Spanish Ministry of Science and Innovation (CTQ2011-29035-C02-02).

References

1- J. M. Dias, M. C. M. Alvim-Ferraz, M. F. Almeida, J. Rivera-Utrilla and M. Sánchez-Polo, J. Environ. Manage., **2007**, 85, 833-846.
2- K. Y. Foo and B. H. Hameed, J. Hazard. Mater., **2010**, 175, 1-11.
3- C. Gabaldón, P. Marzal, A. Seco and J. A. Gonzalez, Sep. Sci. Technol., **2000**, 35, 1039-1053.
4- K. Urano, E. Yamamoto, M. Tonegawa and K. Fujie, Water Res., **1991**, 25, 1459-1464.
5- C. Moreno-Castilla and J. Rivera-Utrilla, MRS Bull., **2001**, 26, 890-894.
6- F. Blanco, X. Vilanova, V. Fierro, A. Celzard, P. Ivanov, E. Llobet, N. Cañellas, J. L. Ramírez and X. Correig, Sens. Actuators, B, **2008**, 132, 90-98.
7- D. Montané, D. Nabarlatz, A. Martorell, V. Torné-Fernández and V. Fierro, Ind. Eng. Chem. Res., **2006**, 45, 2294-2302.
8- K. Okada, N. Yamamoto, Y. Kameshima and A. Yasumori, J. Colloid Interface Sci., **2003**, 262, 194-199.
9- J. Rivera-Utrilla, M. Sánchez-Polo, V. Gómez-Serrano, P. M. Álvarez, M. C. M. Alvim-Ferraz and J. M. Dias, J. Hazard. Mater., **2011**, 187, 1-23.
10- X. Li, Q. Zhang, L. Tang, P. Lu, F. Sun and L. Li, J. Hazard. Mater., **2009**, 163, 115-120.
11- T. Merle, J. S. Pic, M. H. Manero, S. Mathé and H. Debellefontaine, Catal. Today, **2010**, 151, 166-172.
12- J. Rivera-Utrilla and M. Sánchez-Polo, Appl. Catal., B, **2002**, 39, 319-329.
13- M. Sánchez-Polo and J. Rivera-Utrilla, Carbon, **2003**, 41, 303-307.
14- Y.-Z. Zhang, X.-Y. Xiong, Y. Han and W. Zhou, Proc. Environ. Sci., **2011**, 11, Part B, 668-673.
15- M. H. Baek, W. C. Jung, J. W. Yoon, J. S. Hong, Y. S. Lee and J. K. Suh, J. Ind. Eng. Chem., **2013**, 19, 469-477.
16- H. Choi, E. Stathatos and D. D. Dionysiou, Appl. Catal., B, **2006**, 63, 60-67.
17- T. Cordero, C. Duchamp, J. M. Chovelon, C. Ferronato and J. Matos, J. Photochem. Photobiol., A, **2007**, 191, 122-131.
18- G. Li Puma, A. Bono, D. Krishnaiah and J. G. Collin, J. Hazard. Mater., **2008**, 157, 209-219.
19- T. T. Lim, P. S. Yap, M. Srinivasan and A. G. Fane, Crit. Rev. Env. Sci. Technol., **2011**, 41, 1173-1230.
20- J. Matos, A. Garcia, T. Cordero, J. M. Chovelon and C. Ferronato, Catal. Lett., **2009**, 130, 568-574.
21- J. Rivera-Utrilla, M. Sánchez-Polo, M. M. Abdel Daiem and R. Ocampo-Pérez, Appl. Catal., B, **2012**, 126, 100-107.
22- J. L. Figueiredo and M. F. R. Pereira, Catal. Today, **2010**, 150, 2-7.
23- F. Rodríguez-reinoso, Carbon, **1998**, 36, 159-175.
24- W. Wang, C. G. Silva and J. L. Faria, Appl. Catal., B, **2007**, 70, 470-478.
25- I. Velo-Gala, J. J. López-Peñalver, M. Sánchez-Polo and J. Rivera-Utrilla, Appl. Catal., B, **2013**, 142–143, 694-704.
26- I. A. E. A. IAEA. Status of industrial scale radiation treatment of wastewater and its future. (2004).
27- I. A. E. A. IAEA. Nuclear technology review. (2004).
28- I. A. E. A. IAEA. Radiation Processing: Environmental Applications. (2007).
29- I. A. E. A. IAEA. Radiation treatment of polluted water and wastewater. (2008).
30- M. Carballa, F. Omil, J. M. Lema, M. a. Llompart, C. García-Jares, I. Rodríguez, M. Gómez and T. Ternes, Water Res., **2004**, 38, 2918-2926.
31- J. E. Drewes, P. Fox and M. Jekel, J. Environ. Sci. Health, Part A: Toxic/Hazard. Subst. Environ. Eng., **2001**, 36, 1633-1645.
32- L. J. Fono, E. P. Kolodziej and D. L. Sedlak, Environ. Sci. Technol., **2006**, 40, 7257-7262.
33- A. Putschew, S. Wischnack and M. Jekel, Sci. Total Environ., **2000**, 255, 129-134.
34- T. Ternes, Prepr. Ext. Abstr. ACS Natl. Meet., Am. Chem. Soc., Div., **2000**, 40, 98-100.

35- T. Heberer, Toxicol. Lett., **2002**, 131, 5-17.
36- W. Kalsch, Sci. Total Environ., **1999**, 225, 143-153.
37- A. Haiß and K. Kümmerer, Chemosphere, **2006**, 62, 294-302.
38- S. Pérez and D. Barceló, Anal. Bioanal. Chem., **2007**, 387, 1235-1246.
39- M. M. Huber, A. Göbel, A. Joss, N. Hermann, D. Löffler, C. S. McArdell, A. Ried, H. Siegrist, T. A. Ternes and U. Von Gunten, Environ. Sci. Technol., **2005**, 39, 4290-4299.
40- T. A. Ternes, J. Stüber, N. Herrmann, D. McDowell, A. Ried, M. Kampmann and B. Teiser, Water Res., **2003**, 37, 1976-1982.
41- I. Velo-Gala, J. J. López-Peñalver, M. Sánchez-Polo and J. Rivera-Utrilla, Carbon, **2014**, 67, 236-249.
42- E. Atinault, V. De Waele, U. Schmidhammer, M. Fattahi and M. Mostafavi, Chem. Phys. Lett., **2008**, 460, 461-465.
43- G. V. Buxton, C. L. Greenstock, W. P. Helman and A. B. Ross, J. Phys. Chem. Ref. Data, **1988**, 17, 2593-2600.
44- B. G. Ershov, M. Kelm, A. V. Gordeevb and E. Janata, Phys. Chem. Chem. Phys., **2002**, 4, 1872-1875.
45- J. A. LaVerne, M. R. Ryan and T. Mu, Radiat. Phys. Chem., **2009**, 78, 1148-1152.
46- O. Roth and J. A. Laverne, J. Phys. Chem. A, **2011**, 115, 700-708.
47- S. P. Mezyk and D. M. Bartels, J. Phys. Chem. A, **1997**, 101, 6233-6237.
48- G. Fanchini, S. C. Ray and A. Tagliaferro, Surface and Coatings Technology, **2002**, 151-152, 233-241.
49- H. P. Boehm, Carbon, **2012**, 50, 3154-3157.
50- B. Campbell and A. Mainwood, Phys. Status Solidi A, **2000**, 181, 99-107.
51- B. G. Ershov and A. V. Gordeev, Radiat. Phys. Chem., **2008**, 77, 928-935.
52- J. M. Joseph, B. Seon Choi, P. Yakabuskie and J. Clara Wren, Radiat. Phys. Chem., **2008**, 77, 1009-1020.
53- R. Laenen, T. Roth and A. Laubereau, Phys. Rev. Lett., **2000**, 85, 50-53.
54- D. Swiatla-Wojcik and G. V. Buxton, J. Chem. Soc., Faraday Trans., **1998**, 94, 2135-2141.
55- E. A. Voudrias, R. A. Larson and V. L. Snoeyink, Carbon, **1987**, 25, 503-515.
56- I. Velo-Gala, J. J. López-Peñalver, M. Sánchez-Polo and J. Rivera-Utrilla, Chem. Eng. J., **2012**, 195–196, 369-376.
57- R. W. Coughlin and F. S. Ezra, Environ. Sci. Technol., **1968**, 2, 291-297.

Mediterranean Journal of Chemistry

Available free online at www.medjchem.com
Supplementary data
Mediterranean Journal of Chemistry **2015**, 4(2), 68-80

Role of activated carbon on micropollutans degradation by different radiation processes

Inmaculada Velo-Gala, Jesús J. López-Peñalver*, Manuel Sánchez-Polo, José Rivera-Utrilla

Department of Inorganic Chemistry, Faculty of Science, Granada University, Granada, Spain

Table S1. Effect of gamma irradiation on the textural characteristics of ACs.

ACs	S_{BET}[a] (N_2) ($m^2\ g^{-1}$)	V_T[b] (N_2) ($cm^3\ g^{-1}$)	D_P[c] (N_2) (nm)	V_0[d] (N_2) ($cm^3\ g^{-1}$)	S_{Ext}[e] (N_2) (nm)	V_0[f] (CO_2) ($cm^3\ g^{-1}$)	$V_0(N_2)/V_0(CO_2)$
W	815	0.40	1.97	0.35	20.39	0.26	1.36
W – A	798	0.39	1.97	0.35	23.06	0.25	1.40
W – 0	794	0.39	1.97	0.35	20.14	0.24	1.43
C	1294	0.65	2.02	0.55	82.68	0.34	1.60
C – A	1256	0.64	2.03	0.54	71.97	0.33	1.65
C – 0	1248	0.63	2.04	0.53	73.78	0.33	1.62
M	1302	0.66	2.02	0.55	84.00	0.39	1.41
M – A	1286	0.64	1.99	0.54	75.54	0.38	1.43
M – 0	1278	0.63	1.97	0.54	71.16	0.38	1.44
S	1143	0.57	2.02	0.49	53.84	0.29	1.68
S – A	1049	0.52	2.00	0.45	47.48	0.27	1.67
S – 0	1031	0.52	2.03	0.44	53.22	0.28	1.66

[a] Surface area determined from N_2 adsorption isotherms at 77 K.
[b] Total pore volume calculated for $P/P_0 = 0.99$.
[c] Mean pore width determined for a cylindrical model.
[d] Micropore volume determined by the t method.
[e] External surface area calculated by the t method.
[f] Ultramicropore volume based on CO_2 adsorption isotherms at 273 K following Dubinin–Radushkevich equation.

Mediterranean Journal of Chemistry

Available free online at www.medjchem.com
Supplementary data
Mediterranean Journal of Chemistry **2015**, 4(2), 68-80

Table S2. Effect of gamma irradiation on the chemical properties of the ACs.

ACs	pH_{PZC}	Acidic groups[a] (µeq g^{-1})	Basic groups[b] (µeq g^{-1})
W	8.4 ± 0.2	188	403
W-A	9.2 ± 0.2	88	622
W-0	7.1 ± 0.1	128	340
W-H•	4.7 ± 0.1	448	186
W-e^-_{aq}	9.1 ± 0.2	100	558
W-HO•	9.6 ± 0.1	50	688
C	7.5 ± 0.2	240	409
C-A	8.7 ± 0.2	107	657
C-0	7.7 ± 0.2	246	462
C-H•	3.1 ± 0.2	488	158
C-e^-_{aq}	7.2 ± 0.2	166	467
C-HO•	7.7 ± 0.2	226	500
M	10.0 ± 0.2	72	650
M-A	10.7 ± 0.2	90	736
M-0	9.3 ± 0.1	105	468
M-H•	4.2 ± 0.2	453	150
M-e^-_{aq}	8.4 ± 0.2	68	389
M-HO•	9.0 ± 0.2	48	431

[a] Determined by neutralization with NaOH (0.05N).
[b] Determined by neutralization with HCl (0.05N).

Available free online at www.medjchem.com
Supplementary data
Mediterranean Journal of Chemistry **2015**, 4(2), 68-80

Table S3. Atomic percentages of carbon (C1s) and oxygen (O1s) surface obtained by XPS analysis of pristine and modified activated carbon.

C1s						
Type of AC	**AC** [a]	**AC-A** [b]	**AC-0** [c]	**AC-H•** [d]	**AC-e^-_{aq}** [e]	**AC-HO•** [f]
W	95.36	94.90	93.32	94.10	93.52	92.22
C	95.04	92.92	88.01	95.91	94.42	82.55
M	95.34	94.26	94.57	92.01	93.76	93.96
S	95.69	92.97	79.94	95.79	86.13	75.88
O1s						
Type of AC	**AC** [a]	**AC-A** [b]	**AC-0** [c]	**AC-H•** [d]	**AC-e^-_{aq}** [e]	**AC-HO•** [f]
W	3.42	3.90	5.48	4.87	5.46	6.78
C	3.29	4.62	8.05	3.03	4.13	11.18
M	4.14	5.16	4.63	7.11	5.35	5.14
S	4.31	6.55	17.73	3.7	13.87	21.09

[a] Pristine activated carbon.
[b] AC irradiated in the absence of water.
[c] AC irradiated in ultrapure water.
[d] AC irradiated in ultrapure water, pH = 1.0 and $[Cl^-]$ = 1000 mg L^{-1}.
[e] AC irradiated in ultrapure water, pH = 7.5 and $[Br^-]$ = 1000 mg L^{-1}.
[f] AC irradiated in ultrapure water, pH = 12.5 and $[NO_3^-]$ = 1000 mg L^{-1}.

Mediterranean Journal of Chemistry

Available free online at www.medjchem.com
Supplementary data
Mediterranean Journal of Chemistry **2015**, 4(2), 68-80

Table S4. XPS Results: deconvoluted C1s peaks of the XPS spectra for pristine and irradiated carbons.

	Peaks [a] **(**at %**)**						
	1	**2**	**3**	**4**	**5**	**6**	**7**
W	30.71	36.88	11.83	8.38	4.47	4.67	3.06
W-A	50.30	18.81	11.88	6.65	3.76	5.04	3.57
W-0	45.62	19.98	16.54	6.57	3.87	3.91	3.52
W-H•	53.57	16.29	13.84	5.92	3.91	3.48	2.99
W-e^-_{aq}	56.57	8.20	17.39	6.14	4.15	4.56	3.99
W-HO•	50.29	13.99	18.75	5.94	4.48	3.37	3.19
C	33.03	30.32	18.14	6.99	4.93	4.82	1.78
C-A	36.94	26.09	17.46	6.43	3.98	5.33	3.78
C-0	36.19	27.62	16.49	6.67	4.49	5.01	3.54
C-H•	39.68	26.10	16.97	6.20	4.37	4.76	1.92
C-e^-_{aq}	38.13	27.67	16.66	6.69	4.29	4.67	1.89
C-HO•	35.49	28.50	17.57	6.92	5.21	4.70	1.90
M	22.97	35.22	21.56	7.95	3.32	6.67	2.30
M-A	51.50	13.64	12.63	9.15	4.10	5.00	3.98
M-0	51.25	15.14	12.12	9.36	3.85	4.54	3.73
M-H•	38.04	9.79	29.84	10.22	3.94	5.37	2.80
M-e^-_{aq}	40.73	16.43	21.84	8.94	3.70	5.87	2.50
M-HO•	44.36	13.01	22.32	8.50	3.55	5.79	2.46
S	26.73	34.62	14.18	8.97	5.97	4.53	5.00
S-A	42.63	20.17	14.12	8.29	5.23	4.47	5.10
S-0	46.81	18.28	14.78	7.33	4.59	4.74	3.47
S-H•	36.12	18.26	28.95	8.18	4.08	2.42	1.90
S-e^-_{aq}	35.16	17.19	24.71	13.09	5.62	2.82	1.41
S-HO•	38.60	20.58	18.33	12.42	5.38	3.75	0.94

[a] Spectrum calibrated by reference to C1s (284.5 eV). % is percentage of total area. Peaks: 1, C–C bond with sp^2 hybridization; 2, C–C bond of the graphene planes with sp^3 hybridization, C–H; 3, C–O simple bond (alcohol, ether, phenol, and keto–enol); 4, C=O double bond (carbonyl, quinones, and ketones); 5, O–C=O bond in carboxylic acids and anhydrides; 6, π–π* transitions; 7, Plasmon.

Table S5. XPS Results: deconvoluted O1s peaks of the XPS spectra for pristine and irradiated carbons.

Mediterranean Journal of Chemistry

Available free online at www.medjchem.com

Supplementary data

Mediterranean Journal of Chemistry **2015**, 4(2), 68-80

	Peaks [a] **(**at %**)**						
	1	**2**	**3**	**4**	**5**	**6**	**7**
W	31.95	21.27	24.36	11.15	6.07	2.69	2.52
W-A	25.93	21.97	24.36	14.69	6.19	4.10	2.76
W-0	31.05	21.50	21.28	14.51	6.07	2.95	2.63
W-H•	32.93	23.68	21.91	11.11	4.50	2.84	3.03
W-e^-_{aq}	31.24	20.20	21.16	14.77	5.69	2.69	4.24
W-HO•	33.18	25.42	10.35	21.93	5.97	2.23	0.92
C	21.64	22.27	23.54	15.18	12.69	1.62	3.03
C-A	24.25	23.00	22.00	14.48	11.43	1.99	2.84
C-0	28.92	25.31	20.46	14.13	7.64	1.84	1.70
C-H•	26.32	21.78	19.75	18.21	5.63	4.25	4.07
C-e^-_{aq}	22.15	23.66	17.52	20.55	7.55	4.29	4.29
C-HO•	9.6	16.52	21.41	19.62	18.40	10.79	3.66
M	22.63	22.02	15.50	22.63	9.05	4.21	3.96
M-A	25.63	34.17	15.11	15.24	2.70	2.06	5.10
M-0	37.92	20.42	16.84	13.54	6.89	2.31	2.10
M-H•	24.60	25.60	19.95	18.31	6.90	3.04	1.60
M-e^-_{aq}	22.44	20.81	21.89	17.56	9.91	2.92	4.46
M-HO•	24.04	20.10	18.57	21.97	7.81	4.87	2.64
S	39.96	16.46	17.78	12.66	7.16	3.89	2.09
S-A	18.69	26.83	23.36	12.80	11.77	3.24	3.31
S-0	34.93	32.31	18.52	10.03	2.96	1.16	0.09
S-H•	22.33	19.54	24.92	19.58	6.59	4.41	2.63
S-e^-_{aq}	11.80	29.25	17.96	24.55	12.40	3.40	0.64
S-HO•	8.56	29.37	22.83	23.74	11.08	3.29	1.14

[a] Percentage of total area. Peaks: 1, C=O in quinones, carbonyl groups; 2, Oxygen of the carbonyl group (C=O) present in lactones, anhydrides, oxygen atom of hydroxyl groups (–OH); 3, Oxygen atom in lactones and anhydrides (–C–O–C–); 4, Oxygen atom in carboxyl groups (–COOH or COOR); 5, Water or chemisorbed oxygen; 6, Physisorbed water; 7, Plasmon.

Mediterranean Journal of Chemistry

Available free online at www.medjchem.com
Supplementary data
Mediterranean Journal of Chemistry **2015**, 4(2), 68-80

Table S6. Pearson's correlation coefficients for the relationship between E_g value and sp^3/sp^2 ratio.

	sp^3/sp^2 ratio	**Eg**
sp^3/sp^2 ratio		0.5135
Sample Size		(24)
P-Value		0.0103
Eg	0.5135	
Sample Size	(24)	
P-Value	0.0103	

Correlation
(Sample Size)
P-value

This Table shows the Pearson product-moment correlations between the E_g value and sp^3/sp^2 ratio. P-value<0.05 was considered statistically significant at the 95.0% confidence level.